Comprehensive Study on Decoupling Networks for 7 Tesla MRI based on Reactive Load Parasitic-Element

Saana F. Salama[1*], Tareq Baldawi[2], Ashraf Abuelhaija[3], Samer Issa[3]
1- Department of Telecommunication Engineering, Arab American University, Jenin, Palestine.
Email: sanaa.salama@aaup.edu (Corresponding author)
2- Department of Electrical Engineering, Princess Sumaya University for Technology, Amman, Jordan.
Email: thbaldawi@hotmail.com
3- Department of Electrical Engineering, Applied Science Private University, Amman, Jordan.

Received: December 2019 Revised: March 2020 Accepted: May 2020

ABSTRACT:
This work presents and evaluates the integrating of decoupling networks in MRI systems at 7 Tesla magnetic field strength. The parasitic element is reactive loaded. Four different cases of reactive loads are considered: capacitive load, inductive load, open circuited, and short-circuited loads are considered. The idea behind this technique is to reduce or even eliminate the effect of mutual coupling between the RF coil elements in magnetic resonance imaging (MRI)system. Two rectangular loops are used to compose a planar phased array. This structure is designed and optimized in CST at the Larmor frequency of 298.3 MHz corresponding to the 7 Tesla MRI system.

KEYWORDS: Decoupling Network (DN), Matching Network (MN), Parasitic-Element, Capacitive & Inductive Load, Open and Short-Circuited Load.

1. INTRODUCTION

Phased arrays in MRI is a very important issue due to the rapid growth in the MRI techniques [1-2]. The main idea is to enhance the Signal to Noise Ratio (SNR) and shortening the imaging time. By enhancing the SNR, high image resolution is obtained. MRI phased arrays are suffering from the mutual coupling, same as in wireless communications. Mutual coupling mainly reduces the signal to noise ratio and accordingly the image resolution. Recently, solving for the coupling effect in MRI becomes an important issue. In wireless communications, different techniques are proposed to solve the mutual coupling. In [3], lumped and distributed capacitance coupling models between RF coils in MRI system were presented. The idea behind such models is to eliminate the mutual resistance in addition to the mutual reactance for high levels of decoupling. In [4-6], a (DN) circuit of reactive elements is inserted between array active elements was presented based on the eigenmodes theory. While in [7], a reactively loaded parasitic antenna inserted between the two RF coil elements has been proposed. Perfect port isolation was obtained by tuning the parasitic-element parameters but within a narrow band of frequency. In [8], the narrow frequency challenge was solved by changing the reactive load parasitic element with a short-circuited parasitic element and the result was strong port isolation within a larger frequency band. Because of the small separation of the elements ($\approx$ 0.1 of λ), the MRI phased arrays are strongly affected by the mutual coupling. In MRI phased arrays, by decreasing the space between array active elements, the mutual coupling is increasing [9]. Many researchers have been benefited from the designed DNs for wireless communication systems and the same concepts are now applied for MRI phased arrays. In [9], a DN was built based on the idea of reactive load. The reactive loads were modeled as inductive loads connected in parallel with the two RF coil elements in the array. This technique gave good decoupling greater than 23dB over a frequency span [297.931 MHz to 298.23 MHz] and the return loss was (-31.461) dB at frequency of 298.08 MHz. In [10], the idea of parasitic element is applied to achieve high isolation between the RF coil elements. Reference [7] suggested the use of an open circuited parasitic-element. By optimizing the parasitic element parameters and also the active element parameters and lumped element values, good port isolation between the RF coils was obtained with no need for extending the overall area. Over a short range of frequencies [298.21 MHz to 298.34 MHz], an isolation of more than (18) dB was obtained and the return loss was -22.669 dB at a frequency of 298.28MHz.

In this paper, a detailed study of four different cases of parasitic-element based DN for a two elements MRI

Doi: https://doi.org/10.29252/mjee.14.3.6
How to cite this paper: S. Salama, T. Baldawi, A. Abuelhaija, and S. Issa, **"Comprehensive Study on Decoupling Networks for 7 Tesla MRI based on Reactive Load Parasitic-Element"**, *Majlesi Journal of Electrical Engineering*, Vol.14, No. 3, pp. 53-61, 2020.

array will be presented. The coils are the important components in this structure and have to be designed carefully to correctly be matched to the source impedance for maximum power transfer. In this work, the RF coils are designed as rectangular. The coil dimensions and the design details are presented in [11]. Another matching circuit having the L shape is also designed and connected to each RF coil in the two-element array to overcome the matching problem with source resistance of 50 Ω.

This article has the following structure: in Section 2, a parasitic element with capacitive load is designed and optimized. The DN is optimized such that the mutual impedance is very small. While in section 3 the capacitive load is replaced by an inductive load and the DN parameters are optimized to obtain very small mutual impedance between the array RF coils. In sections 4 and 5, an open circuited and short-circuited parasitic element are presented respectively. In all these four different cases of parasitic element based DN, the suggested circuits are tested and optimized at the resonant frequency of the7-T MRI, and the S-parameters of the two rectangular loops array with the DN have been simulated and analyzed. Section 6 discusses the effect of the capacitive load and inductive load values on the S-parameters of the whole structure. In addition, the effect of the series capacitor value, in the L-shaped MN, on the S-parameters is also considered for the other two cases of the open circuited and short-circuited parasitic element-based DN.

2. CAPACITIVE LOAD PARASITIC-ELEMENT BASED DN

Two active element arrays are considered and a capacitive load parasitic-element is placed between the coils. These RF coils of the array are similar and each coil has the shape of rectangular loop RF coil [11], with dimensions of 130 mm × 130 mm. It has been designed to operate at 298.31 MHz corresponding to the resonant frequency of 7-Tesla MRI system. The substrate is made of poly-tetra-fluoro-ethylene, which has a relative permittivity $\varepsilon_r = 2.1$and thickness=12 mm. The width of the microstrip line is 12 mm. The separation between the two RF coils is 10 mm (0.01λ). C_1, C_2 and C_3 are three lumped capacitors distributed along the loop. The matching circuit (L-shaped) is designed as two capacitors (C_{serial}, and C_{shunt}). Between the two active element RF coils, a capacitive load Microstrip Transmission Line (MTL) having length of 170 mm and width of 5 mm is placed representing the parasitic-element with two capacitors connected between the final ends of the 17 cm long transmission line and the ground plane as capacitive load to solve the mutual coupling effect. The whole structure with the decoupling and matching circuit (DMN) is illustrated in Fig.1. This design was simulated using CST software. The impedance matrix shown below relates the terminal voltages and currents [12].

$$\begin{bmatrix} V_1 \\ V_2 \\ V_3 \end{bmatrix} = \begin{bmatrix} Z_{11} & Z_{12} & Z_{13} \\ Z_{21} & Z_{22} & Z_{23} \\ Z_{31} & Z_{32} & Z_{33} \end{bmatrix} \begin{bmatrix} I_1 \\ I_2 \\ I_3 \end{bmatrix} \quad (1)$$

For the parasitic-element and at the terminal point, it is clear that $V_2 = -Z_L I_2$, and according to the reciprocity theorem, $Z_{ij} = Z_{ji}$, knowing that $i \neq j$, $\{i, j = 1,2,3\}$. Putting into (1) and rearranging, then the matrix will be as given in (2):

$$\begin{bmatrix} V_1 \\ V_3 \end{bmatrix} = \begin{bmatrix} Z'_{11} & Z'_{13} \\ Z'_{13} & Z'_{33} \end{bmatrix} \begin{bmatrix} I_1 \\ I_3 \end{bmatrix} \quad (2)$$

Where,

$$Z'_{11} = Z_{11} - \frac{Z_{12}^2}{Z_{22} + Z_L}$$

$$Z'_{33} = Z_{33} - \frac{Z_{23}^2}{Z_{22} + Z_L} \quad (3)$$

$$Z'_{13} = Z_{13} - \frac{Z_{12} Z_{23}}{Z_{22} + Z_L}$$

For identical array elements

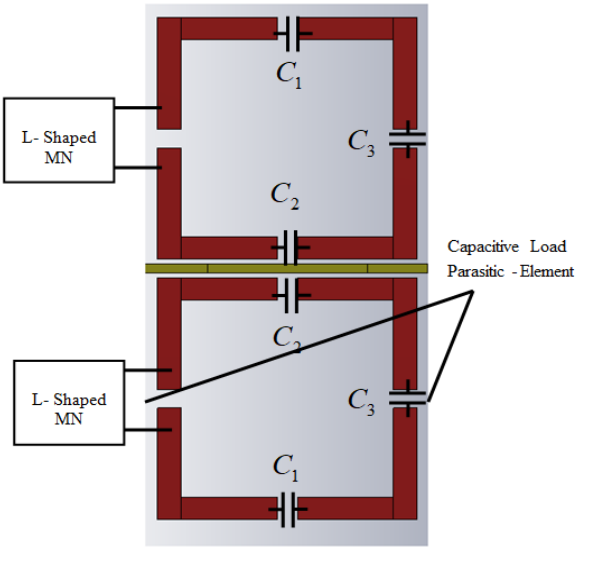

Fig. 1. Two-rectangular loops with a capacitive load parasitic-element based DMN.

$$Z_{12}= Z_{23}$$
$$Z_{11}^{'} = Z_{33}^{'} \quad (4)$$
$$Z_{13}^{'} = Z_{13} - \frac{Z_{12}^{2}}{Z_{22} + Z_{L}}$$

The condition for decoupling ports is $Z_{13}' = 0$, and this requires that Z_{13} must be equal to $Z_{12}^2/(Z_{22}+Z_L)$ and $Z_L = Z_{12}^2 / Z_{13} - Z_{22}$. Adjusting the parasitic-element parameters, the lumped capacitors $C_1, C_2,$ and C_3 and the MN will solve the mutual coupling effect and this leads to strong matching at resonant frequency. After optimization process, the final values are given in Table 1. Using the CST software, the S-parameters of the whole structure with the DMN are simulated. Fig.2 shows a loss of -32.651 dB and an isolation level of 20.706 dB at resonant frequency has been noted.

Table 1. C_1, C_2, and values, DN and MN values.

Lumped Capacitors			***L-Shaped MN***		***DN***	
C_1	C_2	C_3	C_{series}	C_{shunt}	MTL Length/ Width	Capac -itive Load
4.82 pF	4.12 pF	5.5 pF	2.7 pF	12.4 2 pF	17cm/ 0.5cm	1.2 pF

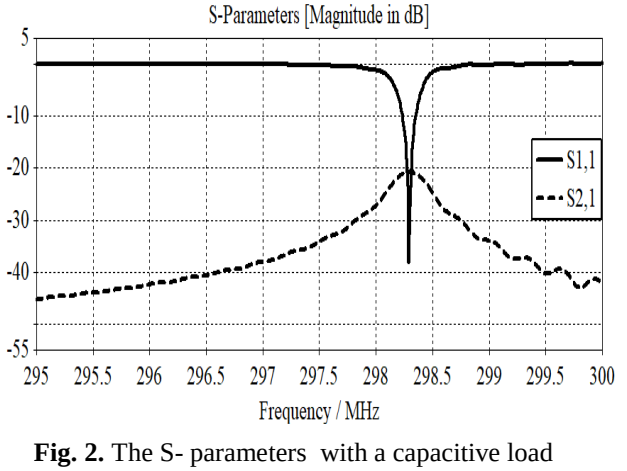

Fig. 2. The S- parameters with a capacitive load parasitic-element based DMN.

In addition, the simulation results of current and magnetic field distribution for the structure with a capacitive load parasitic-element based DMN are shown in Fig.3 at the resonant frequency of 298.3 MHz. Fig.3(a) shows the current magnitude with uniform distribution through the coils without any phase delay. Fig.3(b) shows the magnetic field distribution with a fixed instantaneous amplitude distribution through the coils.

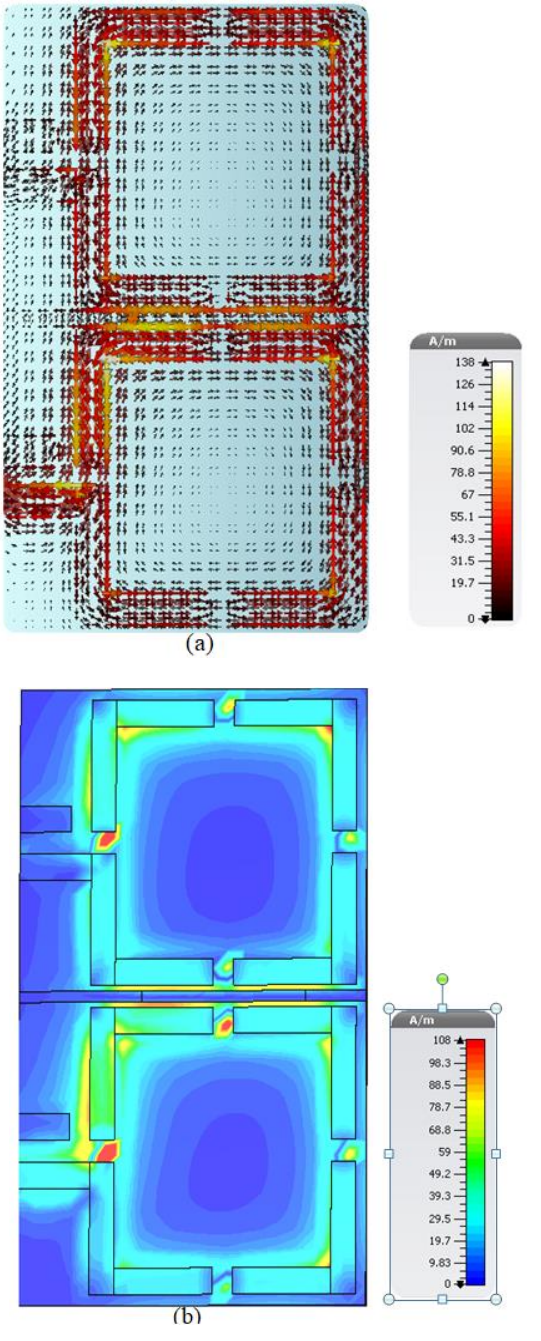

Fig. 3. Simulated results (a) surface current(maximum), and (b) magnetic field at 298.3MHz.

3. INDUCTIVE LOAD PARASITIC-ELEMENT BASED DN

In this case, the capacitive load in Fig.1 is replaced

by an inductive load. Tuning the parasitic-element parameters, the parasitic-element inductive load value, the lumped capacitors distributed along the loop and the MN will give strong matching at the resonant frequency. After the optimization process, all final values are given in Table 2. Fig.4 shows a loss of -26.005dB and an isolation level of 16.029 dB at a frequency of 298.3MHz.

Using simulation, the surface current (as maximum value) and the magnetic field, for this new structure with an inductive load are shown in Fig.5 at the resonant frequency of 298.3MHz. The current magnitude has a uniform distribution through the RF coils. The simulation results of current and magnetic field distributions for the structure are shown in Fig.5 (a) & (b) respectively.

Table 2. C_1, C_2, and values, DN and MN values.

Lumped Capacitors			***L- shaped MN***		***DN***	
C_1	C_2	C_3	C_{series}	C_{shunt}	MTL Length/ Width	Inductive Load
5.1 pF	3.98 pF	5.9 pF	2.3 pF	12.03 pF	17 cm/ 0.5 cm	12nH

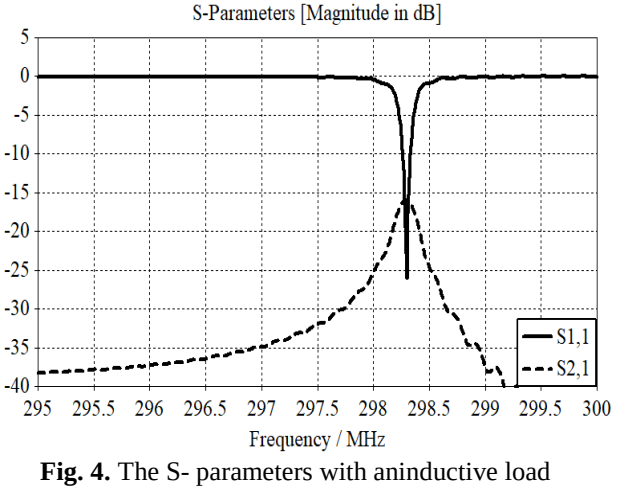

Fig. 4. The S- parameters with aninductive load parasitic-element based DMN.

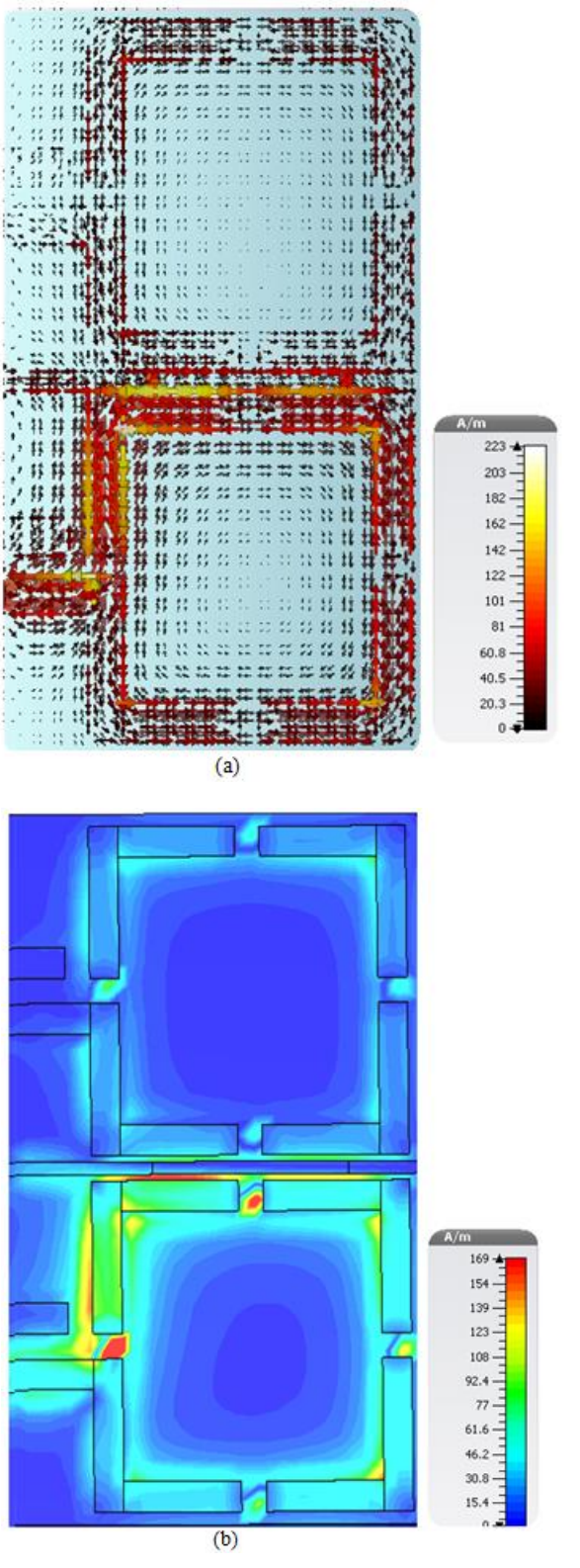

Fig. 5. Result of Simulation, (a) surface current, and (b) magnetic field at 298.3MHz.

4. OPEN CIRCUIT PARASITIC BASED DECOUPLING CIRCUIT

In this case, the insertion of a transmission line (170 mm × 5 mm) with an open circuited end has been used as a parasitic-element between the two rectangular elements. This case was analyzed and considered previously in details by [10], where a loss of -22.669 dB and an isolation level of 18.5311 dB at resonant frequency were obtained as shown in Fig. (6)

The current and magnetic field are shown in Fig.7 at a frequency of 298.28MHz.

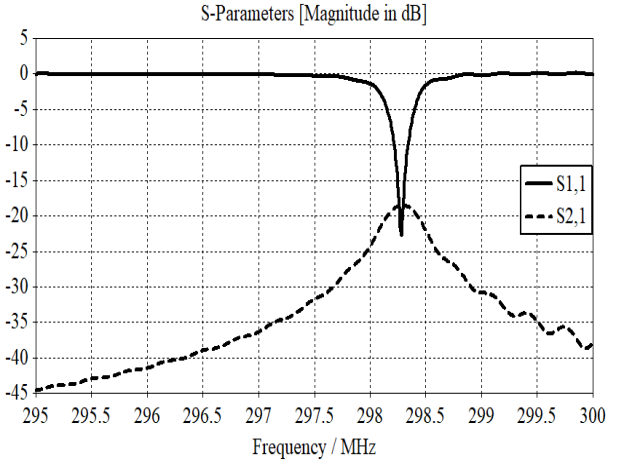

Fig. 6. The simulated S- parameters of the two-rectangular elements with an open circuited parasitic-element based DMN.

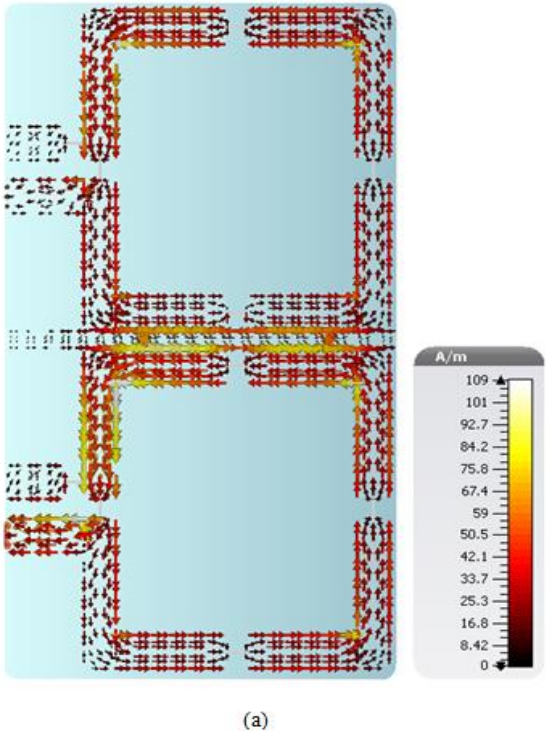

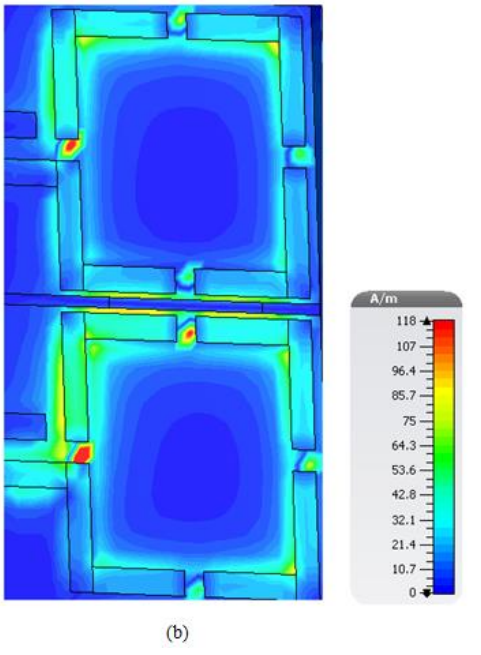

Fig. 7. The simulation results of maximum (a) surface current, and (b) magnetic field at resonant frequency.

5. SHORT CIRCUITED PARASITIC-ELEMENT BASED DN

In this case, the open circuited transmission line in the previous case (Sec. 4) is now short circuited. At the terminal port, the relationship between V, I and Z is given by the following matrix:

$$\begin{bmatrix} V_1 \\ V_2 \\ V_3 \end{bmatrix} = \begin{bmatrix} Z_{11} & Z_{12} & Z_{13} \\ Z_{21} & Z_{22} & Z_{23} \\ Z_{31} & Z_{32} & Z_{33} \end{bmatrix} \begin{bmatrix} I_1 \\ I_2 \\ I_3 \end{bmatrix} \tag{5}$$

In this case, the terminal port is short, this means that $V_2 = 0$, and according to the reciprocity theorem, then $Z_{ij} = Z_{ji}$, knowing that $i \neq j$, $\{i, j = 1,2,3\}$. Putting in (10) and rearranging, the voltages V_1 and V_3 are related with the currents I_1 and I_3 as given in (6):

$$\begin{bmatrix} V_1 \\ V_3 \end{bmatrix} = \begin{bmatrix} Z'_{11} & Z'_{13} \\ Z'_{13} & Z'_{33} \end{bmatrix} \begin{bmatrix} I_1 \\ I_3 \end{bmatrix} \tag{6}$$

Where for identical array elements:

$$\begin{aligned} Z'_{11} &= Z_{11} - \frac{Z_{12}^2}{Z_{22}} = Z'_{33} \\ Z'_{13} &= Z_{13} - \frac{Z_{12}^2}{Z_{22}} \end{aligned} \tag{7}$$

For decoupled ports, the condition $Z'_{13} = 0$ should be fulfilled. Adjusting the parasitic-element parameters, the lumped capacitors and the MN will give strong matching at the resonant frequency of this structure. After optimization process, the final values are summarized in Table 3. Fig.8 shows a loss of -27.822 dB and an isolation level of 35.496 dB at a frequency of 298.3 MHz.

To compare between the four different cases, the return loss, the isolation, and the frequency bandwidth for all cases are sumarized in Table 4. Regards to the return loss, the open and the short circuited parasitic element based DN, the capacitive load parasitic-element based DN, and the inductive load parasitic-element based DN are all well matched at the resonant frequency of 7T MRI. An isolation of approximatly 35 dB is obtained for the case of short circuited parasitic element based DN. While for the case of open circuited, an isolation of approximatly 18 dB is obatained. For the capacitive and inductive load parasitic-element based DN, an isolation of approximatly 20 dB and 16 dB is obtained respectively.

Table 3. C_1, C_2, and C_3 values, DN and MN values.

Lumped Capacitors			***L-Shaped MN***		***DN***	
C_1	C_2	C_3	C_{series}	C_{shunt}	L	W
5.4 pF	4.0 pF	5.84 pF	3.4 pF	12.03 pF	19.4 cm	0.5 cm

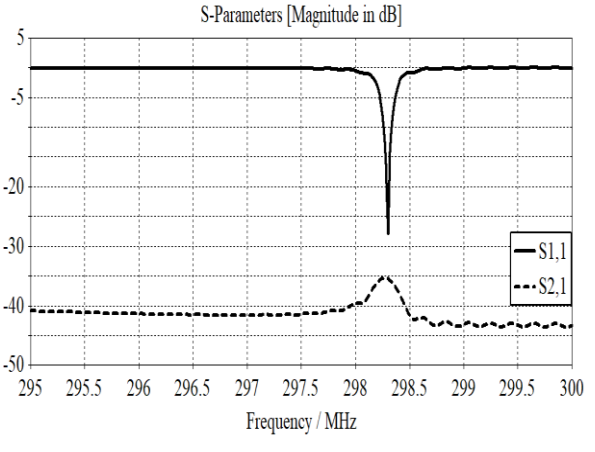

Fig. 8. The simulated S- parameters of the two-rectangular with a short circuited termination.

Table 4. Return loss, isolation, and frequency bandwidth for the four different cases of parasitic element based decoupling circuit.

Parasitic Element Based DN	**Return Loss**	**Isolation**	**Frequency Bandwidth**
Capacitive Load	-32.651 dB	20.706 dB	[298.23 -298.35] MHz
Inductive Load	-26.005 dB	16.029 dB	[298.26 -298.33] MHz
Open Circuited	-22.669 dB	18.531 dB	[298.21 -298.34] MHz
Short Circuited	-27.822 dB	35.496 dB	[298.26 -298.34] MHz

Matching over a narrower frequency range is obtained for the case of inductive load and short circuited parasitic element DN, while matching over a wider frequency range is achieved for the case of capacitive load and open circuited parasitic element based DN.

6. PARAMETRIC STUDY

For the capacitive load parasitic element based DN, the effect of the capacitive load value on the S-parameters has been done using simulation techniques for three values of capacitive load, namely (1*pF*, 1.5*pF*, and 2*pF*). Fig.9(a) and (b) shows the obtained S-parameters .The S-parameter values for the three proposed values of the capacitive load are summarized in Table 5. For capacitive load values of 1.5 *pF* and 2 *pF* , the scatering parameter S_{11} shows mismatching at the resonant frequency and an isolation level of more than (20)*dB* is obtained. But for a capacitive load value of 1 *pF*, S_{11} is correctly matched and an isolation level of more than (20)*dB* is obtained.

As the capacitive load value increases, the resonant frequency decreases.

Also the effect of the inductive load value on the S-parameters is studied for three values of the inductors namely(6 *nH*, 8 *nH*, and 10 *nH*). The obtained S-parameters are shown in Fig.10(a) and (b). The obtained S-parameter values at frequency of 298.3 MHz are summarized in Table 6.

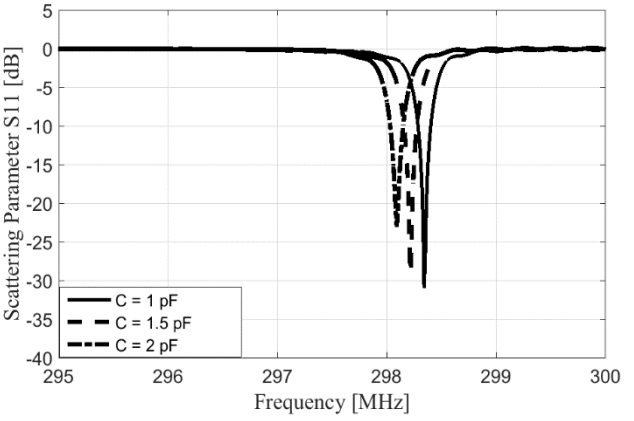

(a)

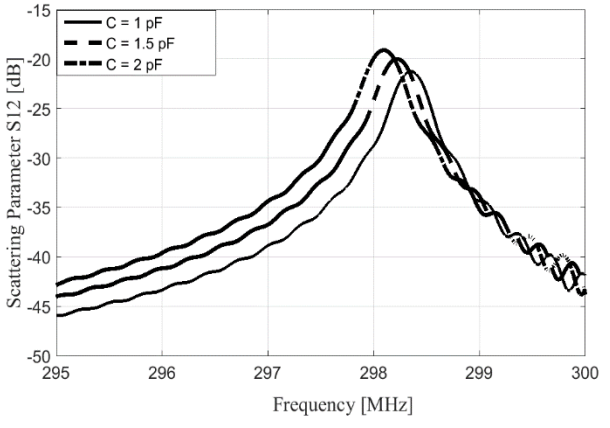

(b)

Fig. 9. The simulation results of S-parameters (a) S_{11} and (b) S_{12} of the two-rectangular elements for three values of the capacitive load .

Table 5. S-parameter values at the resonant frequency for the three proposed values of the capacitive load in the DN.DN

Capacitive Load Value	***S_{11}***	***S_{12}***
1 PF	-12.039 dB	-21.487 dB
1.5 PF	-7.009 dB	-20.569 dB
2 PF	-1.645 dB	-22.855 dB

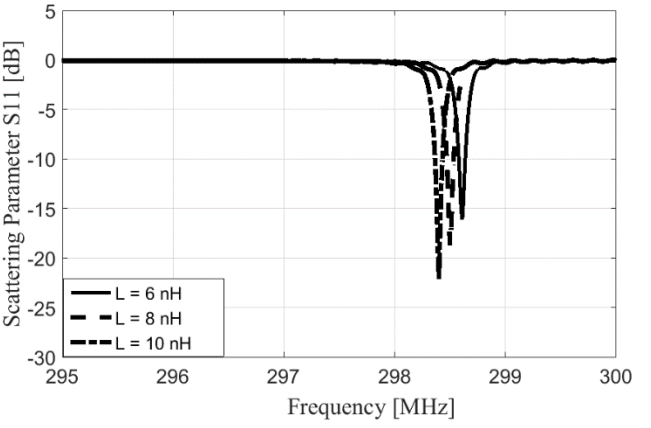

(a)

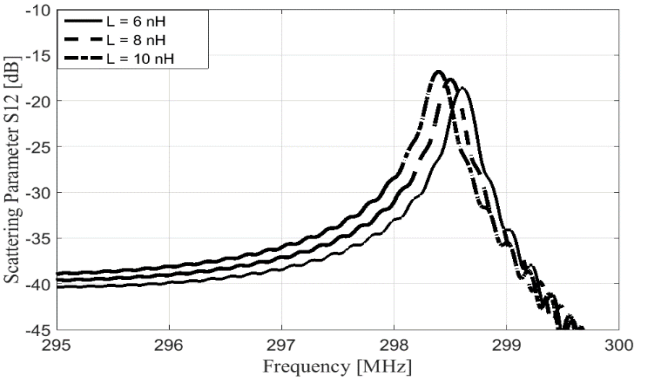

(b)

Fig. 10. The simulation results of S-parameters (a) S_{11} and (b) S_{12} of the two-rectangular elements for three values of the inductors.

Table 6. S-parameter values at the resonant frequency for the three proposed values of the inductive load in the DN

Inductive Load Value	***S_{11}***	***S_{12}***
6 nH	-0.303 dB	-28.475 dB
8 nH	-0.9 dB	-25.053 dB
10 nH	-2.731 dB	-19.381 dB

For inductive load value of 6 *nH*, 8 *nH*, and 10 *nH*, the impedance mismatching occurs at 298.3 MHz and an isolation level of more than 19 *dB* is obtained. Same as capacitive load: by increasing the inductive load value the resonant frequency decreases.

For the open and short circuited parasitic-element based DN, and for the L –shape matching circuit, the effect of the series capacitor value on the S-parameters is studied. For the open circuited parasitic-element, three proposed values of the series capacitor are considered , namely(3 PF, 3.6 PF, and 4.2 PF) with step size of 0.6 pF. The corresponding S-parameters S_{11} and S_{12} are illustrated in Fig.11 (a) and(b) respectively.

Increasing the value of the series capacitor causes the resonant frequency to decrease. For the capacitance value of 4.2 pF, the S-parameter S_{11} becomes mismatched and the decoupling between array active elements decreases by increasing the capacitance.

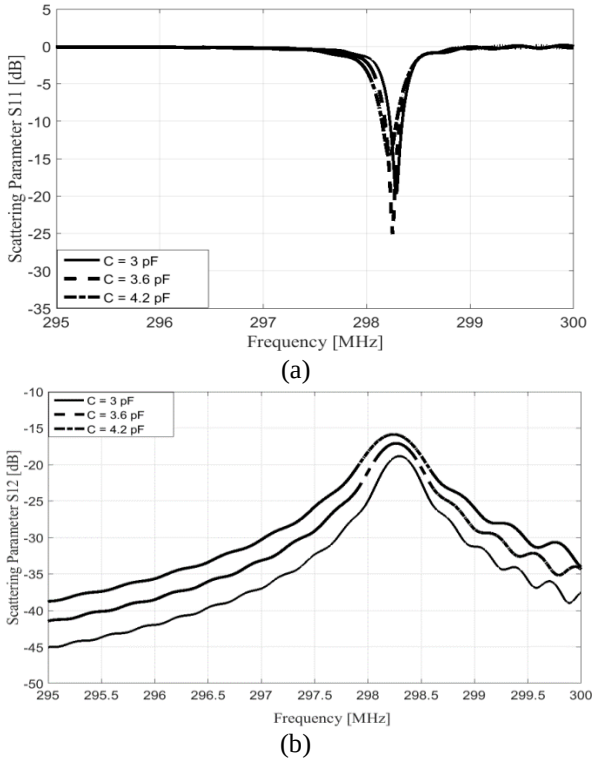

Fig. 11. The simulated S-parameters (a) S_{11} and (b) S_{12} of the two-rectangular elements MRI array for three values of the series capacitor in the L-shaped matching network(case of open circuited parasitic element based DN).

Table 7 summarizes the scattering parameter values at the resonant frequency for three proposed values of the series capacitor in the L-shaped MN.

A comparison has been made between the short circuited parasitic-element based DN and the open circuited case, the S-parameters are calculated for the same values of the series capacitor (3 PF, 3.6 PF, and 4.2 PF) with step size of 0.6 pF. The obtained S-parameters are illustrated in Fig.12 (a) and (b). The resonant frequency f_o is slightly influnced by increasing the capacitance value of the series capacitor in the L-shaped MN. The parameter S_{11} gave better matching at the capacitance value of 3.6 pF and an isolation level greater than (30) dB is obtained for the three capacitance values. Table 8 summarizes the S-parameter values at the resonant frequency for the three proposed values of the series capacitor.

Table 7. The obtained S-parameters at 298.3 MHz for three proposed values of the series capacitor in the L-shaped MN.

Series Capacitor Value	***S_{11}***	***S_{12}***
3 PF	-18.279 dB	-18.847 dB
3.6 PF	-13.264 dB	-17.155 dB
4.2 PF	-9.279 dB	-16.028 dB

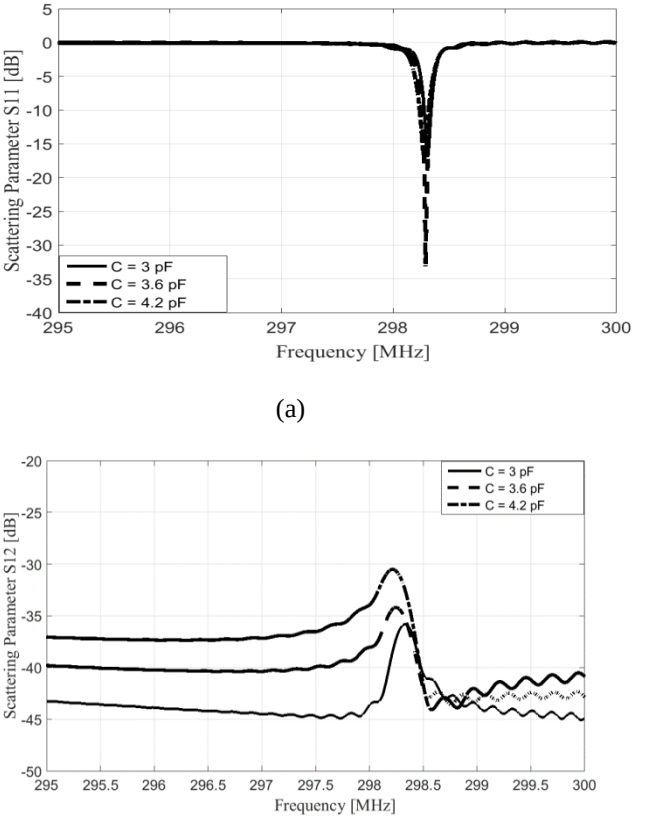

Fig. 12. The simulated S- parameters (a) S_{11} and (b) S_{12} of the two-rectangular elements MRI array for three values of the series capacitor in the L-shaped MN (case of short circuited parasitic element based DN).

Table 8. The obtained S-parameters at 298.3 MHz for three proposed values of the series capacitor in the L-shaped MN.

Series Capacitor Value	S_{11}	S_{12}
3 pF	-15.651 dB	-35.971 dB
3.6 pF	-26.498 dB	-34.597 dB
4.2 pF	-14.319 dB	-31.493 dB

7. CONCLUSION

In this work, four different cases of parasitic-element based DN are presented. For the capacitive load based DN, a loss of -32.651 dB and an isolation level greater than 20 dB are achieved at 298.3MHz. For the case of inductive load based DN, the loss of -26.005 dB and an isolation level greater than 16 dB are achieved. For the open circuited based DN, the loss was -22.669 dB and an isolation level greater than (18) dB are achieved. For the short-circuited based DN, the loss was (-27.822) dB and an isolation level greater than 35 dB are achieved. The maximum isolation level is obtained in the case of short-circuited parasitic-element based DN. Matching over a wider frequency bandwidth is obtained in the case of open circuited parasitic-element based DN. The surface current and magnetic field have been simulated for the four different cases of the parasitic-element based DNs.

In addition, the effect of the capacitive and inductive load values on the S-parameters of the whole system have been demonstrated. The effect of the series capacitor value of the L-shaped MN on the S-parameters for the cases of open and short circuited parasitic-element is also considered.

For future work, the coupling among RF coils in MRI phased array becomes difficult to be handled with more elements placed in a given area. The design of decoupling networks for 4-channel array and above is a good idea to be studied in a future work.

REFERENCES

[1] D. K. Sodickson, and W. J. Manning, **"Simultaneous Acquisition of Spatial Harmonics (SMASH): Fast Imaging with Radiofrequency Coil Arrays,"** *Magn. Reson. Med.,* pp. 591–603, Vol. 38, No. 4, Oct. 1997.

[2] P. B. Roemer, W. A. Edelstein, C. E. Hayes, S. P. Souza and O. M. Mueller, **"The NMR Phased,"** *Magn. Reson. Med.*, pp. 192–225, Vol. 16, No. 2, Nov.1990.

[3] M. Maunder and et al., **"Stray Capacitance Between Magnetic Resonance Imaging Coil Elements: Models and Application to Array Decoupling,"** *IEEE Transactions on Microwave Theory and Techniques*, Vol. 61, No. 12, December 2013.

[4] J. C. Coetzee, and Y. Yu, **"Closed-form design equations for decoupling networks of small,"** *Electronics Letters*, Vol. 44, No. 25, Dec. 2008.

[5] P. T. Chua, and J. C. Coetzee, "**Microstrip decoupling networks for low order multi-port arrays with reduced element spacing**", *Microwave and Optical Technology Letters*, pp. 592-597, 2005.

[6] S. Salama, and K. Solbach, "**Design of decoupling network for monopole four square array antenna for multi-beam applications**," *LAPC 2013*, Loughborough, UK, Nov. 2013

[7] K. Lau, and J. B. Andersen, "**Simple and efficient decoupling of compact arrays with parasitic scatterers**," *IEEE Transactions on Antennas and Propagation*, Vol. 60, No. 2, February 2012.

[8] S. Salama, and K. Solbach, "**Parasitic Elements Based Decoupling Technique for Monopole Four Square Array Antenna**", *European Microwave Conference EuMC2014*, Rome, Italy, October 2014.

[9] S. Salama, "**Reactive-Element Based Decoupling Network for a Two Element MRI Phased Array**", *Journal of King Saud University Engineering Sciences JKSU*, May 2018. (accepted).

[10] S. Salama and A. Abuelhaija, "**Parasitic-Element Based Decoupling Network for a Two Element MRI Phased Array**," *JEEIT 2019*, Amman, Jordan, April. 2019.

[11] S. Salama, "**Design of a Rectangular Loop-Shape RF Coil for 7-Tesla Magnetic Resonance Imaging**," *APMC 2017*, Kuala Lumpur, Malaysia, Nov. 2017.

[12] M. Pozar D. M., **Microwave Engineering**. Hoboken, NJ, USA: Wiley, 2005.